

# Reduction of Sensitivity to Measurement Errors in the Derivation of Equivalent Models of Emission in Numerical Computation

Xin Tong, David W. P. Thomas, Angela Nothofer, Christos Christopoulos, and Phillip Sewell

George Green Institute for Electromagnetics Research  
University of Nottingham, Nottingham, NG2 7RD, UK  
vanppp@gmail.com, dave.thomas@nottingham.ac.uk, angela.nothofer@nottingham.ac.uk,  
phillip.sewell@nottingham.ac.uk, christos.christopoulos@nottingham.ac.uk

**Abstract** — In this paper, the accuracy of an equivalent dipole model for representing electromagnetic emissions from printed circuit boards (PCB) is studied. The optimization of near-field measurement parameters and required PCB parameters for building a numerical model are discussed and their impact on the accuracy of emission predictions is examined.

**Index Terms** — Error analysis, near field scanning, numerical modelling, radiated fields.

## I. INTRODUCTION

Predicting electromagnetic emissions from PCBs is an important topic in electromagnetic compatibility (EMC) studies and product designs. Simulation techniques based on equivalent models have many advantages compared to the full field simulations. The heavy task of modeling the complexity of PCBs and the huge computational costs to solve the model are alleviated. In addition, detailed information on circuit structure is not needed to model emissions from PCBs by equivalent sources. This ensures simplicity, confidentiality of designs and facilitates the task of design engineers.

A method to represent radiated emissions from a PCB using an equivalent dipole model deduced from a magnetic near-field scan was described in [1]. Modeling techniques in both open and closed environments were considered. A PCB is modeled with a set of equivalent magnetic dipoles placed on the component surface. The ground plane is also explicitly included in the model based on

certain approximations in order to simulate the emissions in the whole space. In closed environments, the method is extended to include dipoles, dielectric, and conducting plane (DDC model) to explicitly represent the physical presence of the PCB. Thus, the major interactions between the PCB and enclosure are taken into account. The equivalent dipoles are identified by fitting the measured tangential magnetic near fields to the fields generated by the dipoles. The modeling process can then be described as:

1. Take a near field scan of the transverse magnetic fields emitted by the PCB.
2. Through solving the inverse problem (see equation (4)) find the equivalent dipoles for the PCB.
3. Model the PCB in the environments of interest (enclosures or free space) to predict its performance.

Figure 1 shows the simple test board used where comparisons with full 3D simulations are required. The configuration used for the basic test board is given in Table 1 and typical results are shown in Fig. 2.

For the near-field scanning based method, measurement parameters (scanning surface, sampling, distance, error analysis, etc.) have noticeable effects on the accuracy of associated modeling and simulation. Optimization of measurement parameters not only improves the efficiency of near-field scanning, but also reduces the modeling errors possibly introduced from

measurements. An early overview of determination of measurement parameters can be found in [2]. The sampling and scan-plane reduction techniques are developed from the electromagnetic propagation theory in [3] and [4], respectively. In [5, 6], extensive error analysis for near-field measurements is performed using measurement tests, simulation tests, and mathematical analysis. For the proposed method, it is essential to specifically optimize the parameters of the required planar near-field measurements based on the electromagnetic theory and measurement or simulation tests, as well as to have an error budget of the numerical modeling and associated measurements.

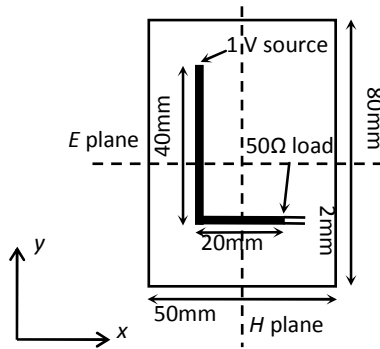


Fig. 1. Geometry of the basic test board (top view).

Table I: Configuration of near-field measurement with the test board

frequency (GHz)	1
scanning plane height (mm)	11.5 above the PCB
scanning plane size (mm)	120 × 75
scanning resolution (mm)	2.5
sampling points	49 × 31

In this paper, the optimization of the near-field measurement parameters for the model is discussed. Finally, error and uncertainty in the numerical modeling and associated measurements are examined. With these studies, the objective is to develop the methodology of modeling electromagnetic emissions using equivalent dipoles deduced from near-field scanning as completely as possible, and to show how the

technique described here meets the needs for predictive work in EMC studies.

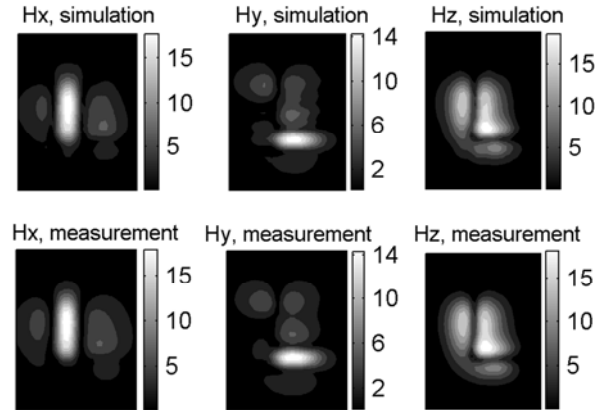


Fig. 2. Magnetic fields (mA/m) in the scanning plane at 1 GHz. Top row) simulation based on equivalent dipoles; bottom row) measurement.

## II. EFFECTS OF MEASUREMENT PARAMETERS

For the near-field scanning based method, the measurement parameters have noticeable effects on the accuracy of modeling and simulation. Knowledge of these effects helps to determine the choice of measurement configuration. Scanning resolution, scanning plane area, and SNR are critical parameters in near-field sampling. To study this, a far-field simulation in the E plane for the basic test board is repeated using the equivalent dipole method with different measurement parameters, and the correlation coefficient between results obtained by the equivalent dipole simulation and the full field simulation is introduced as a measure of accuracy. The correlation coefficient is defined as:

$$\gamma = \frac{\sum_{i=1}^N (E_i - \bar{E})(E'_i - \bar{E}')}{\sqrt{\sum_{i=1}^N (E_i - \bar{E})^2 \sum_{i=1}^N (E'_i - \bar{E}')^2}} \quad (1)$$

where  $E_i$  is the dipole equivalent result set,  $E'_i$  is the full field simulation result set,  $\bar{E}_i$  and  $\bar{E}'_i$  are the averages of  $E_i$  and  $E'_i$ , respectively, and  $N$  is the number of samples. All full field simulations are performed with a method of moment (MoM) based solver Concept – II 9.4 [7, 8].

### A. Scanning resolution

According to the information theory, the scanning resolution is a key factor in acquiring sufficient near-field information. In the examples above, a 2.5 mm resolution is used for both PCBs. This is based on the sampling criterion recommended by Joy and Paris [3] which estimates the maximum spacing between sampling points ( $\Delta s$ ) allowed to obtain sufficient information for planar near-field scanning as:

$$\Delta s = \frac{\lambda}{2\sqrt{1+(\lambda/d)^2}}, \quad (2)$$

where  $\lambda$  is the wavelength and  $d$  is the separation distance between the EUT and the probe. The maximum spacing allowed for the test boards considered according to (2) is 5.7 mm and 6.0 mm, respectively. So the choice of 2.5 mm is reasonable. To validate this criterion, the far field prediction of the test board is repeated with the same set of near-field data but of different resolutions, and the correlation coefficient with full field simulation is shown in Fig. 3. The results from near-field data of 2.5 and 5 mm resolution make very little difference and are close to the direct simulation result, as they are within the range of maximum space allowed. But the data with a 10 mm resolution and above has obvious inaccuracies as indicated by the lower correlation. This confirms the criterion for the choice of sampling points that any space sampling less than the maximum spacing allowed in (2) is sufficient.

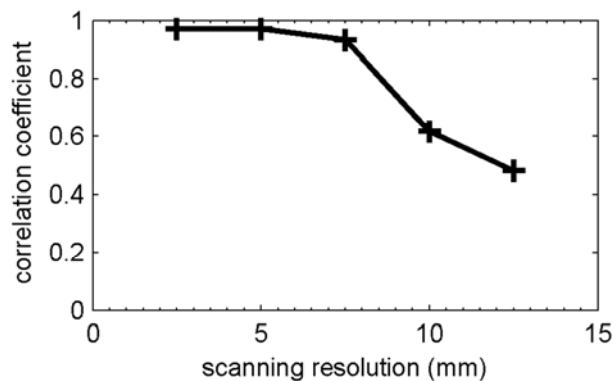


Fig. 3. Effects of scanning resolution.

### B. Scanning plane area

Another important topic with regard to near-field sampling is the size of scanning plane. Unlike the modal expansion method, the method presented here does not assume the field outside the scanning area to be zero. The equivalent sources are established by fitting to the measured near-field data. Therefore if any significant field area is not covered in the near-field scanning plane, some information will be lost and the equivalent sources established from it would have a noticeable error. It is well known that magnetic near-field maps from a PCB are dominated by the fields vertically above the board and gradually become weaker as the sampling point extends outward to the perimeter of the PCB [9, 10]. This implies that the scanning area must at least cover the area of the PCB, and could possibly extend beyond it. Ideally, the scanning plane should extend until the field on the edges of the plane reaches the minimum measurable level (noise floor) of the equipment. But in practice it is not necessary to scan so widely in order to collect sufficient near-field information. Based on our studies, a near-field plane where the maximum field on the edges is approximately 20 dB lower than the overall maximum field is required. Figure 4 shows the effects of scanning the area size on the far field prediction for the test board. It is found that insufficient scanning information (when there is 5 and 10 dB maximum – edge difference) results in significant inaccuracies, but the far field is correctly predicted when the scanning plane reaches a large enough size (19 and 28 dB maximum – edge difference).

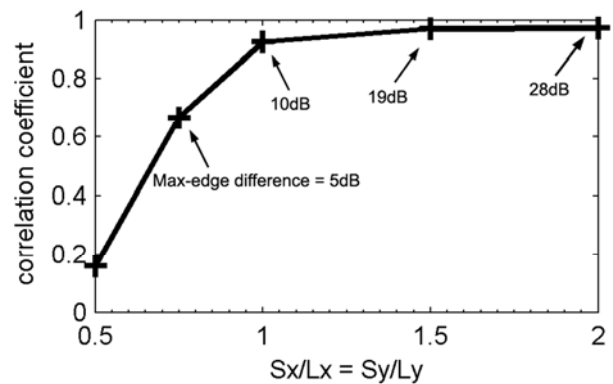


Fig. 4. Effects of scanning area.  $S_x$ ,  $S_y$ : length of the scanning plane in x and y direction, respectively.  $L_x$ ,  $L_y$ : length of the PCB in x and y direction, respectively.

Actually, the plane area required to satisfy this criterion is not very large. In the case above, a 19 dB maximum – edge difference corresponds to a plane which is 1.5 times of the PCB dimension ( $100 \times 75$  mm). This result also implies that when a scanning plane is large enough, further increasing its size does not significantly improve the accuracy of the equivalent source method.

### C. Substrate permittivity

Knowledge of the permittivity of the PCB substrate is needed when constructing the complete DDC model for simulations in closed environments. The most accurate way is to measure it experimentally, but not every EMC lab has the required equipment. Normally, PCB manufacturers provide general information on the substrate. In practice, the actual value may differ due to manufacturing uncertainties, constructional details, etc. It is therefore necessary to establish how accurate the value of permittivity should be for inclusion in the model. As a quantitative study, the vertical electric field along two orthogonal lines within an enclosure at a non-resonant frequency (1 GHz) is predicted with equivalent models built with different values of permittivity, and the correlation coefficients with results obtained from full field simulation are shown in Fig. 5. The typical value of the substrate permittivity is 4.6 (FR4). The predicted field is in an acceptable range provided that the permittivity value used for modeling is within 20% of the actual value. This implies that an accurate enough model can be built for most EMC studies as long as the general type of the dielectric substrate is known.

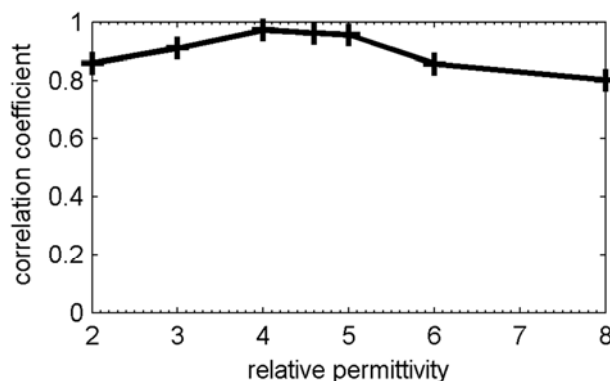


Fig. 5. Effects of modeled permittivity value.

## III. ERROR AND UNCERTAINTY

### A. Measurement errors

The errors due to the measurement system are recognized as the major error source of near-field techniques. Generally, there are three categories of error source, related to the probe  $\delta_p$ , receiver  $\delta_r$ , and test conditions  $\delta_t$ . The probe related errors include positioning error, antenna factor error, and multiple reflection error. The 3D positioner in our scanning system has a mechanical precision of 10  $\mu\text{m}$  in  $x$ ,  $y$ , and  $z$  direction which is much smaller than the RF wavelength, so the probe positioning error can be considered negligible. The antenna factor error depends on the probe's polarization properties relative to those of the EUT. This error is examined by two methods: a) experiments where the ratio of the primary and cross-polar components of a known field coupled to the probe is measured [11], and b) simulations where a probe of typical dimensions and structure subject to an incident arbitrary but known field is modeled to find out its polarization properties. The two studies give similar results that a typical probe parameter error with our setup at RF frequencies is approximately  $\delta_{p1} \leq 0.15$  dB. The errors due to multiple reflections between the scanned PCB and probe are examined from simulations. An infinite ground plane and a loop probe of typical dimensions are modeled to represent the possibly largest reflections. Based on the simulation, a typical upper bound of multiple reflections error at RF frequencies is approximately  $\delta_{p2} \leq 0.1$  dB.

Errors related to the receiver (arising from dynamic range, nonlinearity, mismatch, systematic random errors, etc.) and test conditions have been extensively studied by other authors [5, 6]. Based on their studies and the performance of our equipment (HP E8362B [12]), the two categories of errors have upper bounds  $\delta_r \leq 0.25$  dB and  $\delta_t \leq 0.1$  dB. If the errors are assumed to be independent, according to the central limit theorem the total error budget in near-field scanning for PCBs with our measurement system can be estimated as

$$\delta = \sqrt{\sum \delta_i^2} \leq 0.35 \text{ dB.} \quad (3)$$

## B. Numerical accuracy

The effects of measurement errors on the calculated dipoles through the numerical computation are examined here. The moments of the equivalent dipoles are numerically determined from the inverse problem of a linear equation system

$$\xi \cdot \bar{M} e^{i\bar{\theta}} = \bar{H} e^{i\bar{\phi}}, \quad (4)$$

where  $\xi$  is the coefficient matrix,  $\bar{M}$  and  $\bar{\theta}$  are vectors of the amplitude and phase of equivalent dipoles, and  $\bar{H}$  and  $\bar{\phi}$  are vectors of the amplitude and phase of measured magnetic fields.  $\xi$  has exact values but  $\bar{H} e^{i\bar{\phi}}$  contains inevitable errors  $\overline{\Delta H}$  and  $\overline{\Delta \phi}$ , leading to errors in the resulting dipole moments. The linear equation system becomes:

$$\xi \cdot (\bar{M} e^{i\bar{\theta}} + \overline{\Delta M}) = (\bar{H} + \overline{\Delta H}) e^{i(\bar{\phi} + \overline{\Delta \phi})} = [\bar{H} e^{i\bar{\phi}} + \overline{\Delta H} e^{i\overline{\Delta \phi}}] e^{i\bar{\phi}}. \quad (5)$$

The right-hand side can be Taylor expanded with only terms of first and second order retained.

$$\xi \cdot (\bar{M} e^{i\bar{\theta}} + \overline{\Delta M}) = \bar{H} e^{i\bar{\phi}} + (\overline{\Delta H} + i\bar{H}\overline{\Delta \phi} + i\overline{\Delta H}\overline{\Delta \phi} - \bar{H}\overline{\Delta \phi}^2/2) e^{i\bar{\phi}}. \quad (6)$$

From (4) and (6), we can obtain

$$\overline{\Delta M} = \xi^{-1} \cdot (\overline{\Delta H} + i\bar{H}\overline{\Delta \phi} + i\overline{\Delta H}\overline{\Delta \phi} - \bar{H}\overline{\Delta \phi}^2/2) e^{i\bar{\phi}}, \quad (7)$$

$$\|\overline{\Delta M}\| = \|\xi^{-1}\| \cdot \|(\overline{\Delta H} + i\bar{H}\overline{\Delta \phi} + i\overline{\Delta H}\overline{\Delta \phi} - \bar{H}\overline{\Delta \phi}^2/2) e^{i\bar{\phi}}\|. \quad (8)$$

From (4), we can also obtain

$$\|\xi\| \cdot \|\bar{M} e^{i\bar{\theta}}\| \geq \|\bar{H} e^{i\bar{\phi}}\|. \quad (9)$$

Therefore, the upper bound of relative error in the equivalent dipoles due to measurement errors can be expressed by combining (8) and (9) as

$$\frac{\|\overline{\Delta M}\|}{\|\bar{M} e^{i\bar{\theta}}\|} \leq \text{cond}(\xi).$$

$$\frac{\|(\overline{\Delta H} + i\bar{H}\overline{\Delta \phi} + i\overline{\Delta H}\overline{\Delta \phi} - \bar{H}\overline{\Delta \phi}^2/2) e^{i\bar{\phi}}\|}{\|\bar{H} e^{i\bar{\phi}}\|}, \quad (10)$$

where  $\text{cond}(\xi) = \|\xi^{-1}\| \cdot \|\xi\|$  is the condition number of the matrix  $\xi$  [13].  $\overline{\Delta H}$  and  $i\bar{H}\overline{\Delta \phi}$  in the right hand side represent the dominant error terms in measured magnitude and phase, respectively. Due to the fact that the condition number of a matrix is always  $\geq 1$ , the small errors in measurement may be magnified in the resulted equivalent dipole array. Mathematically this situation is called an ill-conditioned equation system. In order to keep a high numerical accuracy, numerical methods such as the L-curve method and singular valued decomposition [14] have to be applied to solve the equations.

## C. Uncertainty tests

Efficient computational techniques are expected to avoid the measurement errors being magnified in the resulted equivalent dipole array. But it is still worth examining to what extent the measurement errors (with a typical upper bound 0.35 dB) would affect the accuracy of the model. To study this, the far field of the basic test board is predicted with near-field data with different levels of normally distributed noise as well as a reference with no intentionally added noise. As the noise is randomly generated, the results may differ from one time to another. Figure 6 shows an example illustrating the general idea. A standard deviation 0.35 dB of the measured near field leads to an uncertainty  $\pm 1$  dB in the far field prediction. As a comparison, a greater error of a standard deviation 1 dB leads to a larger uncertainty ( $\pm 2$  dB). Particularly, most uncertainties occur in places where the field intensity is relatively weak. Measurement errors are magnified from near-field data to the predicted far fields.

Equation (10) links the possibly largest overall errors to a number of factors. Our tests suggest that experimental errors are of the order of 0.35 dB and that overall errors are of the order of 1 dB. This confirms the magnification of errors as indicated by (9) which in our case is a factor of the order of 0.7 dB ( $\times 1.2$ ). This factor will vary depending on the choice of sampling points, the technique for numerically solving the equation system, etc. as indicated by the various terms in (9). The discussion following (9), gives some

guidance as to the impact of various solution techniques to the problem accuracy. Results published for predicted fields in enclosures [1] show similar accuracy although errors in the definition of the enclosure will also contribute to the error budget.

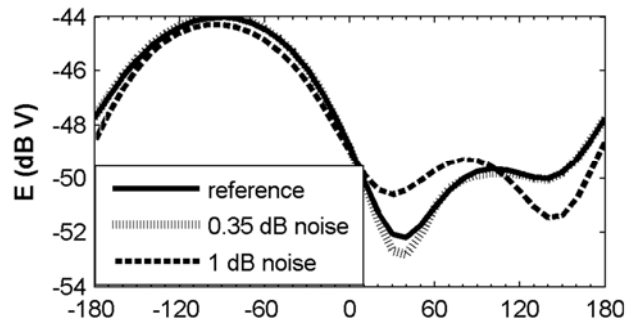


Fig. 6. Far-field patterns calculated from data with different levels of noise.

#### IV. CONCLUSION

Verification and validation studies of the equivalent dipole model for predicting electromagnetic emission from PCBs are presented. Case studies with two test boards show the validity of the model in both free space and enclosed environments. The optimization of near-field measurement parameters and their impact on prediction accuracy are demonstrated. It has been shown that the inclusion of basic structural details of ground plane and substrate in addition to the equivalent dipoles permit fairly accurate prediction of emitted fields to be made not only in free space but also in enclosures that have interactions with the PCBs inside.

Generally, the method has better performance in free space than in enclosed environments. This may be attributed to the greater degree of approximations made to the model in enclosed environments. The real current distribution of the PCB is also assumed to be the same in free space and enclosed environments. This may be true in most but not all cases. In a highly populated enclosure (several PCBs in close proximity), stronger interactions may be present and the model may display a lower accuracy. Nevertheless, we have demonstrated that the proposed techniques have the potential to characterize emissions from complex structures in realistic environments reducing computational effort significantly and

making it possible to perform complete system EMC studies.

Future work will look at more complex multilayered and double sided PCBs where board resonance effects are more noticeable [15]. Evaluation of the application of these measurement uncertainties to other field solvers will also be investigated [16].

#### ACKNOWLEDGMENT

The work was supported by the EPSRC UK Grant No: EP/D048540/1.

#### REFERENCES

- [1] X. Tong, D. W. P. Thomas, A. Nothofer, P. Sewell, and C. Christopoulos, "Modeling Electromagnetic Emissions From Printed Circuit Boards in Closed Environments Using Equivalent Dipoles," *IEEE TRANS. ON EMC*, vol. 52, no. 2, pp. 462-470, May 2010.
- [2] A. D. Yaghjian, "An Overview of Near-Field Antenna Measurement," *IEEE Trans. Antennas Propagat.*, vol. AP-34, pp. 30-45, Jan. 1986.
- [3] E. B. Joy and D. T. Paris, "Spatial Sampling and Filtering in Near-Field Measurements," *IEEE Trans. Antennas Propagat.*, vol. AP-20, pp. 253-261, May 1972.
- [4] D. J. Van Rensburg, "Scan-Plane Reduction Techniques for Planar Near-Field Antenna Measurements," *IEEE Trans. Antennas Propagat.*, vol. 46, no. 6, pp. 179-184, Dec. 2004.
- [5] A. C. Newell, "Error Analysis Techniques for Planar Near-Field Measurements," *IEEE Trans. Antennas Propagat.*, vol. 36, no. 6, pp. 754-768, Jun. 1988.
- [6] A. C. Newell and C. F. Stubenrauch, "Effect of Random Errors in Planar Near-Field Measurement," *IEEE Trans. Antennas Propagat.*, vol. 36, no. 6, pp. 769-773, Jun. 1988.
- [7] A. F. Peterson, S. L. Ray, and R. Mittra, "Computational Methods for Electromagnetics," Wiley: IEEE Press, 1997.
- [8] Concept - II homepage. [Online]. Available: <http://www.tet.tu-harburg.de/concept/index.en.html> (2009)
- [9] R. G. Kaires, "Radiated Emissions from Printed Circuit Board Traces Including the Effect of Vias, as a Function of Source,

Termination, and Board Characteristics," *IEEE International Symposium on EMC*, pp. 872–877, 1988.

- [10] R. Garg, P. Bhartia, I. Bahl, and A. Ittipiboon, *Microstrip Antenna Design Handbook*. Norwood, MA: Artech House, 2001.
- [11] D. W. P. Thomas, K. Biwojno, X. Tong, A. Nothofer, P. Sewell, and C. Christopoulos, "Measurement and Simulation of the Near-Field Emissions from Microstrip Lines," in *Proc. EMC Europe 2008*, pp. 1-6, Sep. 2008.
- [12] HP E8362B User's Guide, Hewlett-packard Co. Santa Rosa, CA, 2000.
- [13] G. Allaire, S. M. Kaber, "Numerical Linear Algebra," New York: Springer, 2008.
- [14] P. C. Hansen, "Numerical Tools for Analysis and Solution of Fredholm Integral Equations of the First Kind," *Inverse Problem* 8, pp. 849-872, 1992.
- [15] S. Kahng, "Predicting and Mitigating Techniques of the PCB Rectangular Power/Ground Planes' Resonance Modes," *Applied Computational Electromagnetic Society (ACES) Journal*, vol. 22, no. 3 pp. 15-23, Nov. 2007.
- [16] J. Carlsson, P-S. Kildal, "User-Friendly Computer Code for Radiated Emission and Susceptibility Analysis of Printed Circuit Boards," *Applied Computational Electromagnetic Society (ACES) Journal*, vol. 14, no. 1, pp. 1-8, March 1999.



**Xin Tong** was born in Hunan, China, in December 1984. He received the B.Sc. degree in Engineering Physics from Tsinghua University, Beijing, China, in 2006. He is currently working toward the Ph.D. degree in Electronic Engineering at the University of Nottingham, Nottingham, UK.

His research interests include modeling and experimental methods in electromagnetic compatibility (EMC), more particularly the characterization of emissions.



**David W. P. Thomas** received the B.Sc. degree in Physics from Imperial College of Science and Technology, the M.Phil. degree in Space Physics from Sheffield University, and the Ph.D. degree in Electrical Engineering from Nottingham University, in 1981, 1987 and 1990, respectively. In 1990 he joined the Department of Electrical and Electronic Engineering at the University of Nottingham as a Lecturer where he is now an Associate Professor and Reader in Electromagnetic Applications. His research interests are in power system transients, power system protection, electromagnetic compatibility and electromagnetic simulation. He is a member of CIGRE and convenor for JWG 4.207



**Angela Nothofer** was born in Uelzen, Germany, in 1967. She received the Dipl.-Ing. degree in Electrical Engineering from the University of Hannover, Germany, in 1995, and the D.Phil. degree in Electronics from the University of York, U.K., in 2001.

In 2000, she joined the National Physical Laboratory, U.K., where she developed standards and methods for measuring electromagnetic field strength as a member of the RF & Microwave Team. Her main research was in EMC measurement methods above 1 GHz using GTEM cells and fully anechoic rooms (FAR).

In 2005, she joined the George Green Institute for Electromagnetics Research (GGIEMR) at the University of Nottingham as a Lecturer in Electromagnetic Applications. Her main research areas are electromagnetic compatibility (EMC), and RF and microwave measurements using TEM waveguides, fully anechoic rooms, and reverberation chambers.



**Christos Christopoulos** was born in Patras, Greece in 1946. He received the Diploma in Electrical and Mechanical Engineering from the National Technical University of Athens in 1969 and the M.Sc. and

D.Phil. from the University of Sussex in 1979 and 1974, respectively.

In 1974, he joined the Arc Research Project of the University of Liverpool and spent two years working on vacuum arcs and breakdown while on attachments at the UKAEA, Culham Laboratory. In 1976, he joined the University of Durham as a Senior Demonstrator in Electrical Engineering Science. In October 1978, he joined the Department of Electrical and Electronic Engineering, University of Nottingham, where he is now Professor of Electrical Engineering and Director of the George Green Institute for Electromagnetics Research (GGIEMR).

His research interests are in Computational Electromagnetics, Electromagnetic Compatibility, Signal Integrity, Protection and Simulation of Power Networks, and Electrical Discharges and Plasmas. He is the author of over 400 research publications and seven books and seven chapter contributions in books. He has received the Electronics Letters, the Snell Premium and the Measurement and Technology Premium by the IET and several conference best paper awards. He is a member of the IET and an IEEE Fellow. He is past Executive Team Chairman of the IEE Professional Network in EMC and Associate Editor of the IEEE EMC Transactions. He is Chairman of URSI Commission E on the Electromagnetic Environment and Interference and Fellow of the Royal Academy of Engineering.



**Phillip Sewell** received the B.Sc. degree in Electrical and Electronic Engineering (first-class honors) and Ph.D. degree from the University of Bath in 1988 and 1991, respectively.

From 1991 to 1993, he was a Post-Doctoral Fellow with the University of Ancona, Ancona, Italy. In 1993, he became a Lecturer with the School of Electrical and Electronic Engineering, University of Nottingham, Nottingham, U.K. In 2001 and 2005, he became a Reader and Professor of Electromagnetics at the University of Nottingham.